Molecular Current−Voltage Characteristics

Jorge M. Seminario,*,† Angelica G. Zacarias,† and James M. Tour*,‡

Department of Chemistry and Biochemistry, University of South Carolina, Columbia, South Carolina 29208, and Department of Chemistry and Center for Nanoscale Science and Technology, Rice University MS-222, 6100 Main Street, Houston, Texas 77005

Received: May 14, 1999

A density functional theory calculation for determining the I−V characteristics (admittances of molecules) in molecular-based junctions is presented here. The efficacy of this method is shown by calculations of $I(V)$ characteristics on an S−(p-C_6H_4)−S between proximal Au atoms and comparing the data to the results obtained experimentally. Over the range studied experimentally, the calculations here corroborate well with the $I(V)$ characteristics found in molecular junction experiments.

Recently, Reed et al. performed measurements of $I(V)$ characteristics on molecular junctions using benzene-1,4-dithiolate between proximal Au probes which permitted the quantization of electronic transport at the molecular level.[1] Currents on the order of 0.2 μA at 5 V were reported through the molecular junctions yielding a driving point admittance of 40 nanoΩ^{-1}. That work followed a series of measurements on atomic and molecular systems using scanning tunneling microscopes (STM) and other techniques.[2−4] The ability to precisely determine the $I(V)$ characteristics, which are usually termed conductance measurements, of a molecule is critical for the development of molecular scale electronics, and theoretical work is becoming a powerful research complement for guiding these studies.[3,5−14] Moreover, theoretical work can aid in determining the intrinsic electronic effects of the molecule. Following the results of Reed et al.,[1] we have performed here a series of theoretical calculations on the transfer of charge through molecular junctions in a systematic manner from very simple systems up to the system used in the experiment using for the first time quantum chemistry techniques wherein the calculated current can be presented in terms of $I(V)$, just as in the measured values. These calculations show the complicated nature of the electron conduction through single molecules, which cannot be represented with a lump parameter as in standard circuit theory. Therefore, these calculations can serve as a primary guide for future atomistic circuits in the burgeoning field of molecular scale electronics.

Density functional theory (DFT) techniques[15−18] were used for all systems. The functionals used are Perdew−Wang 91 for correlation and Becke-3 for exchange (B3PW91).[19,20] The basis set used was the double-split D95[21] combined with effective core potentials.[22] Presently, this seems to be the most powerful combination of tools to deal with relatively large numbers of very heavy atoms. The use of the pseudopotentials with relativistic corrections has been widely demonstrated to be a good compromise with the alternative use of full-electron procedures. This reduces the required computational effort without loss of accuracy.[23] The basis set used for the Au atom is the Los Alamos National Laboratory (LANL) set for effective core potentials (ECP) of double-ζ type.[22] The hybrid functional B3PW91, where a portion of the exchange functional is calculated as a fully nonlocal functional of the wave function of an auxiliary noninteracting system of electrons resembles the exchange in the Hartree−Fock (HF) procedure (actually in any wave function procedure), is commonly referred to as a DFT−HF hybrid. However, it should be considered that the so-called exchange is being calculated using a noninteractive wave function whose density, but not its wave function, corresponds to the real system. A detailed analysis of the hybrid schemes and their theoretical rigor was recently reviewed.[24] All calculations were performed using the Gaussian-94 program.[25] All geometry optimizations were performed via the Berny algorithm in redundant internal coordinates.[26] The threshold for convergence was 0.00045 atomic units (au) and 0.0003 au for the maximum force and root-mean-square force, respectively. The self-consistency of the noninteractive wave function was performed with a requested convergence on the density matrix of 10^{-8}, and 10^{-6} for the RMS and maximum density matrix error between iterations. These settings provide correct energies of at least five decimal figures and geometries of an accuracy of around three decimal figures within the level of theory used.

The effect of the external voltage applied to the molecule is performed by an external electric field applied in the direction of the axis of the molecule, and this simulates the voltage applied to the molecule. For example, when an external field is applied to the system (Au−molecule−Au or Au−atom−Au), the charge transferred from the Au atoms on one side to the Au atoms on the other side is calculated by a Mulliken population procedure, and the time that it takes for this transfer is calculated using an approximated Fermi Golden Rule,[27] which is based on standard time-dependent perturbation theory. The initial and final states in this analysis are the many-electron wave functions of the system (Au plus molecule) when no field and a field, respectively, are applied to the system. These two eigenvalue problems are solved using quantum DFT techniques available in the Gaussian-94 program. We used the B3PW91 functional; however, any of the other sophisticated fully correlated methods can be used as well. The picture below illustrates the calculation process. Calculations are performed when no external field is applied, then when an external field is applied. The Hamiltonians H_0 and H_V include the Au atoms in the ab initio calculation since the molecule is in contact with one, two, or at most three

† University of South Carolina.
‡ Rice University.

10.1021/jp991570s CCC: $18.00
Published on Web 09/10/1999

Au atoms. These are point contacts; thus, the effects of the bulk metal are minimally detected by the adsorbates at a 1−3 atom atomic cluster (as in the break junction experiment[1] where the tips are also of atomistic dimensions). Including the Au atoms and molecule under study in the real Hamiltonian, i.e., dealing with real electrons instead of quasiparticles, circumvents problems connected with one electron phenomenological Hamiltonians, semiempirical input data, classical image charge effects, and self-energies, as well as the determination of contact Fermi energies, since all such information is embedded in the real many-electron Hamiltonian. A population analysis allows us to obtain the charges Q_0's at each end when no external electrical field is applied to the system. The charge is identical at each end since we are using symmetrical systems in the *z*-direction. Then, charges Q_1 and Q_2 are calculated when the external potential is applied. For the system without the external voltage applied, we have the Schrödinger equation written as

$$H_0\Psi_0 = E_0\Psi_0 \tag{1}$$

where $\Psi_0(r_1,r_2,...,r_N)$ is the many-electron wave function, which

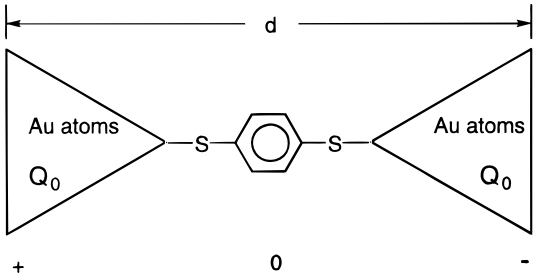

includes electrons in the gold atoms, and E_0 is the total energy of the system. The charge in both Au atoms is Q_0. The Schrödinger equation, when the external field is applied, is given by

$$H_V\Psi_V = E_V\Psi_V \tag{2}$$

where $\Psi_V(r_1,r_2,...,r_N)$ is the *n*-electron wave function when the

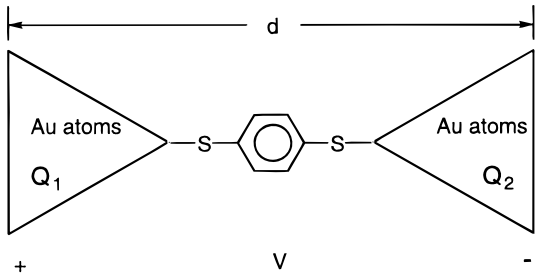

external potential V is applied and E_V is the total energy of the system. The charges $Q_1 > Q_2$ are those obtained due to the effect of the external potential V.

The Hamiltonian for the molecule without the external field is given by

$$H_0 = -\frac{1}{2}\sum_{i}^{N}\nabla_i^2 - \sum_{A=1}^{M}\sum_{i=1}^{N}\frac{Z_A}{R_{Ai}} + \sum_{i=1}^{N-1}\sum_{j=i+1}^{N}\frac{1}{r_{ij}} + \sum_{A=1}^{M-1}\sum_{B=A+1}^{M}\frac{1}{R_{AB}} \tag{3}$$

and the Hamiltonian for the molecule under the external field has one extra interaction term

$$H_V = H_0 + \frac{V}{d}\sum_{i=1}^{N} z_i = H_0 + V_1 \tag{4}$$

where V is a constant external potential and d is the distance along the axis of the molecule. Therefore, using the charges and the transition rate W_{V0}, we can obtain the current I.

$$I = \frac{\Delta Q}{\Delta t} \tag{5}$$

where

$$\Delta Q = Q_1 - Q_0 \tag{6}$$

$$\Delta t = \frac{1}{W_{V0}} \tag{7}$$

and W_{V0} is approximated by

$$W_{V0} = \frac{2\pi}{\hbar}|\langle\Psi_V|V|\Psi_0\rangle|^2\rho(E_0 - E_V) \tag{8}$$

where $\rho(E_0 - E_V)$ is approximated to be constant in the region of interest and proportional to the energy difference between initial and final state. The charge transferred was calculated by a population analysis followed by a time-dependent perturbation approach to determine the transfer rates. We tried the Mulliken[28] population analysis and the ChelpG,[29] which yielded nearly identical results. Given the simplicity of the Mulliken population analysis, we chose it to account for the transferred electron charge in all the calculations.

Before studying the benzene-1,4-dithiolate system, we decided to test the charge transfer through an atomic system, namely Xe. Experimental results on Xe have been reported by Yazdani et al.[4] using a surface of Ni and a STM tip of W. Therefore, the Au-based results with this calculation would not be expected to be comparable. To analyze the effect of the surrounding Au atoms on the tips without and with the Xe atom, we have chosen the following systems: Au−Au at equilibrium distance, Au−Xe−Au at equilibrium distance, Au···Au at the Au−Au distance in the Au−Xe−Au system, and the Au_3−Xe−Au_3 system where the Xe resides above the center of the two Au-based tripods. The Au−(*p*-C_6H_4)−Au was also studied in order to have a systematic analysis of the Au−S−(*p*-C_6H_4)−S−Au system. Experimental information is only available for the latter configuration. The geometries are shown in Figure 1, together with their Au−Au internuclear distances (these distances are equivalent to the Au−Au internuclear distance used by Reed et al.[1]) These structures were fully optimized at the level of B3PW91/LANL2DZ.

Figure 2A shows the charge transfer versus the applied external electric field between two Au atoms bridged by a Xe atom and the case where the Xe resides above the center of the two Au-based tripods. For the case of the Au trimers at each side, the charge transfer is very smooth as the electric field is increased. There is a region of linear behavior for small external fields, dropping to a value close to zero slope when the external field parallel to the direction of the Au atoms is between 0.012 and 0.024 au. After this region, the transferred charge increases again linearly up to a value 0.05 au for the electric field (last points calculated are not shown in the figure) where the total charge transferred corresponds to three electrons. To compute the total charge transferred in the case of the triangular Au clusters, we have added the charge in the three Au atoms.

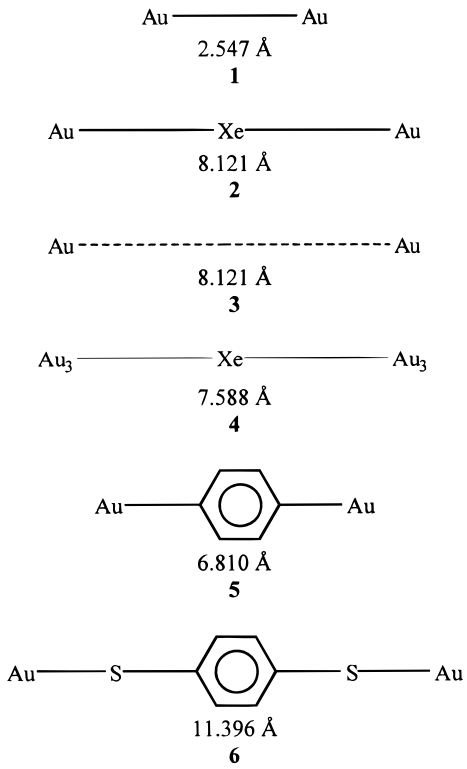

Figure 1. Systems analyzed (indicating the optimized Au−Au distances). Notice that **5** and **6** are also represented as Au−(*p*-C_6H_4)−Au and Au−S−(*p*-C_6H_4)−S−Au, respectively. All systems were treated as both singlets and triplets. Results reported correspond to the lowest energies, i.e., **1** and **5** were closed-shell singlets, and **2**, **3**, **4**, and **6** were open-shell triplets under the DFT.

For the electron charge transferred from one Au atom to the other through a Xe atom, the plot shows three regions (Figure 2A). The first region, where little charge is transferred, increases up to an external field of 0.008 au. The second region shows a linear increase of the charge transferred and goes up to 0.03 au of external field applied parallel to the axis Au−Xe−Au. At this point, there is a sudden increase in the charge transferred of about 0.02 au (data not shown). After this point, the increase of charge continues with approximately the same slope as the slope of the first region. The charge transfer on this system is always smaller than the case with the Au trimers and electron transfer becomes worse as the excitation external electric field increases. Our calculations cover the range from zero to three transferred electrons. These calculations also show that the Mulliken charge in the Xe atom is practically zero during the charge transfer process. In addition, we have analyzed the electron transfer of the same system when no Xe atom is connected between the two Au tips; that is, the two Au atoms were set at the distance they would have been if the Xe atom were present. We find that there is not charge transfer until the applied field is about 0.1 au (not shown in the figure), and at this point, the transferred charge suddenly jumps from zero to become identical to the transferred charge for the case when the Xe is present. This indicates a full tunneling effect through the metallic ends as opposed to the partial tunneling in the case of the Au−Xe−Au and no tunneling in the case of the Au_3−Xe−Au_3 system. Therefore, Au_3−Xe−Au_3 shows a totally different behavior than the one with a single Au at each end. The main difference is that the system with the Au_3 clusters on each side does not show the threshold for charge transfer as in the Au−Xe−Au system. This is an indication that the Au atoms

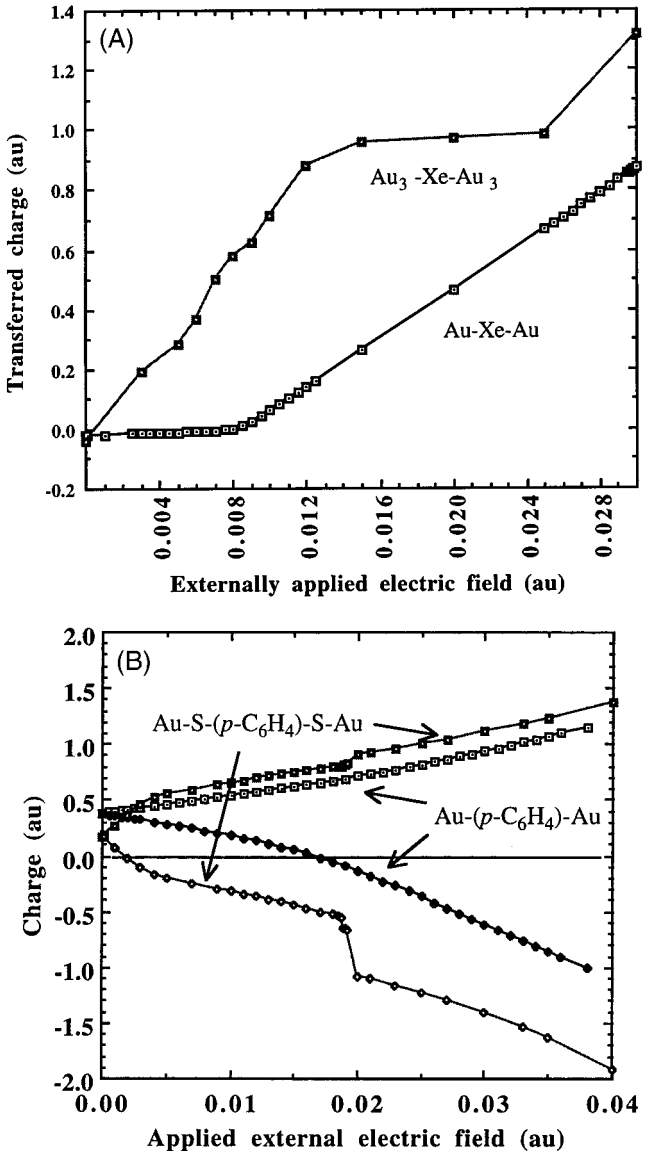

Figure 2. (A) The charge transferred from one Au atom to the other Au atom in a Au−Xe−Au system and from one Au_3 cluster to the other Au_3 cluster in the Au_3−Xe−Au_3 system as a function of the external applied field. (B). The charge transferred from one Au atom to the other in Au−(*p*-C_6H_4)−Au and Au−S−(*p*-C_6H_4)−S−Au as a function of the externally applied electric field in the direction along the Au atoms. The charge in the donor Au atom corresponds to the positive side, and the charge in the acceptor Au atom corresponds to the negative side.

around the bridge atom play an important and determinant role in the conduction measurements.

The transfer of electrons through a *p*-phenylene moiety between two Au atoms is shown in Figure 2B. The data look very similar to the transfer over simply two Au atoms except that the Au−Au is not shifted by 0.4 electrons as in the case of the *p*-phenylene-containing system. The main difference between the Au−(*p*-C_6H_4)−Au and the case with just two Au atoms is that, with the former system, the Au atoms have a positive charge at equilibrium. Figure 2B also shows the results for the Au−S−(*p*-C_6H_4)−S−Au system, the configuration as described by Reed et al.[1] The sulfur atoms were required in the experiment for the thermodynamically driven self-assembly process. The charge is transferred between the Au atoms; however, the carbon/sulfur atoms have more participation in the charge transfer than Xe had in the case of the Au−Xe−Au system.

The transfer to the Au atom also shows three regions and a larger sudden change in the charge transfer around the 0.02 au of external field excitation where the charge transferred increases by approximately half an electron. We expect that this corresponds approximately to the HOMO−LUMO gap of the molecule. The charge transfer in the Au−S−(*p*-C_6H_4)−S−Au system increases linearly until a full electron is transferred out from the donor Au atom.

Figure 3 shows how the electron densities along axes parallel to the axis of symmetry of the molecule change when the external field induces a transfer of one electron from one Au atom to the other. Figure 3A shows that, when one electron has been transferred from one Au atom to the other, the electron density close to the axis of the molecule undergoes little, if any, change, and the two curves (with and without the field) are coincident, even when one electron has been transferred. However, at 1.5 Å from the axis of symmetry, a slight change can be noticed as shown in Figure 3B. A stronger change is observed at 3 Å from the axis of symmetry as shown in Figure 3C; around the first Au atom, the electron density has decreased almost totally and a strong increase is observed around the second Au atom. These plots indicate that the charge transfer affects the exterior of the systems at about 2−3 Å from the axis of symmetry. This is of major importance considering that the Au−Au distance on a surface of Au(100) is approximately 2.88 Å.[30]

Finally, Figure 4A−C shows the *I*(*V*) curves for all cases studied using the approximations indicated for eq 8. The variations of the current are strongly dependent on the input voltage and they possess strong nonlinear behavior. Figure 4A shows the *I*(*V*) behavior for currents on the order of 1 mA. As expected, the best conductance in this range corresponds to the case of the Au−Au system. The Au−Xe−Au follows, then the aryl systems. Remarkably, in the range of tenths of microamps (Figure 4B), where the experiments of Reed et al.[1] were performed, the conductances of the Au−S−(*p*-C_6H_4)−S−Au and Au_3−Xe−Au_3 become greater than those of the Au−Au. Figure 4B also shows the experimental results.[1] The curve "exp1" is the reported *I*(*V*) characteristic for one molecule together with the "exp2" which was assumed to correspond to having two molecules in parallel that were noninteracting. In Figure 4B, "2*exp1" is simply the mathematical doubling of exp1. Therefore, the difference between "exp2" and "2*exp1" gives us an indication of the error bars in the experiment; hence, the theoretical results here are within the tolerance yielding a good agreement between theory and experiment in the 0−3 V range. After 3 V, the experimental results show several varying oscillations; therefore, a comparison cannot be made after 3 V of applied external voltage. However, another explanation could be suggested by the present calculations. Possibly the molecule of "exp1" is connected to only one Au atom on each side; this connection is sufficiently weak so that after 3 V the system becomes unstable. However, the curve "exp2" may also correspond to one molecule but connected to two or three Au atoms at each end. This makes a stronger connection and yields a larger current as expected. Figure 4C shows the results for very small currents. Here, the Au−S−(*p*-C_6H_4)−S−Au system yields higher conductances than the other cases. This is the range of values where molecular scale electronic current-based circuits would most likely be used: currents in the range of nanoamps and voltages below 1 V.

Over the range studied experimentally, the calculations here corroborate well with the *I*(*V*) characteristics found in the molecular junction experiment[1] wherein tenths of microamps were observed over a few volts. Therefore, the utility of these quantum chemistry techniques for computing the *I*(*V*) characteristics of molecular-based systems is demonstrated.

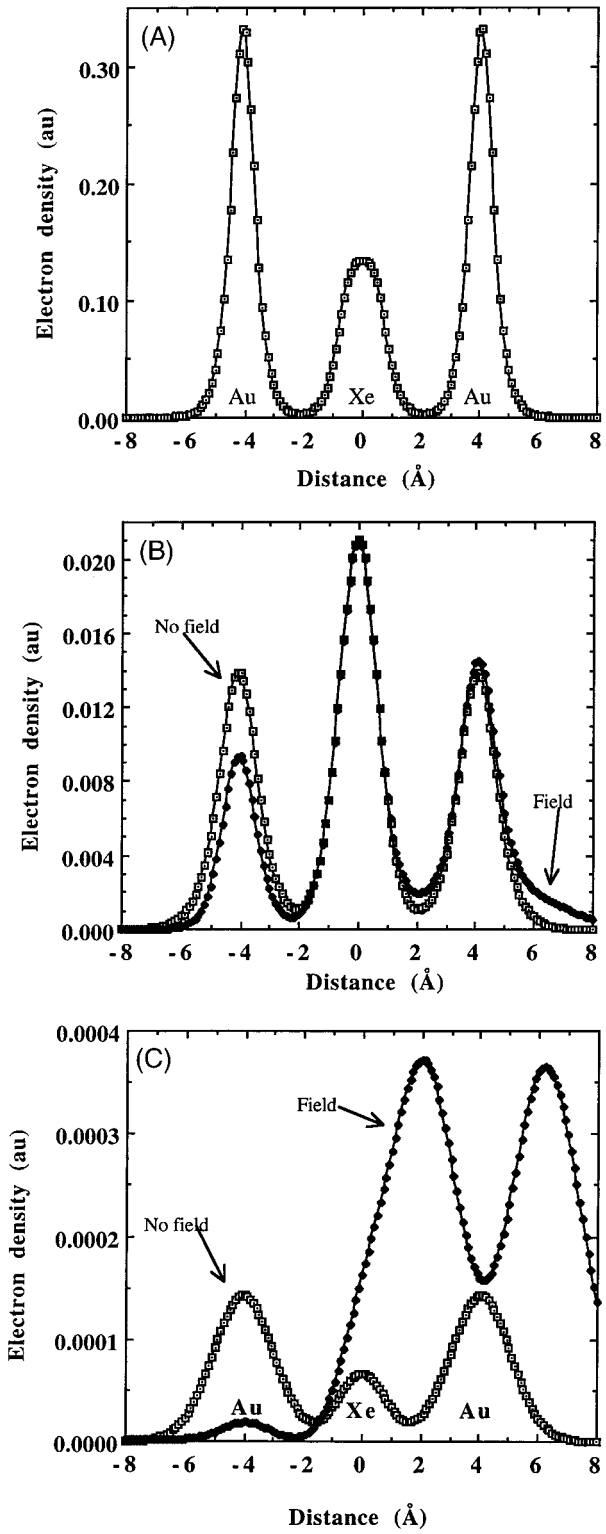

Figure 3. The electron densities along axes parallel to the Au−Xe−Au axis showing the effect of the external applied field when one electron is transferred from the Au atom on the right side of the junction to the Au on the left side (A) at 0.8 Å, (B) at 1.5 Å, and (C) at 3 Å from the Au−Xe−Au axis, respectively.

In summary, we have been able to use DFT techniques for the study of charge conductance through molecules. It was found that the position of the molecule, with respect to the Au atoms, has a strong effect on the charge transfer. If the molecule is

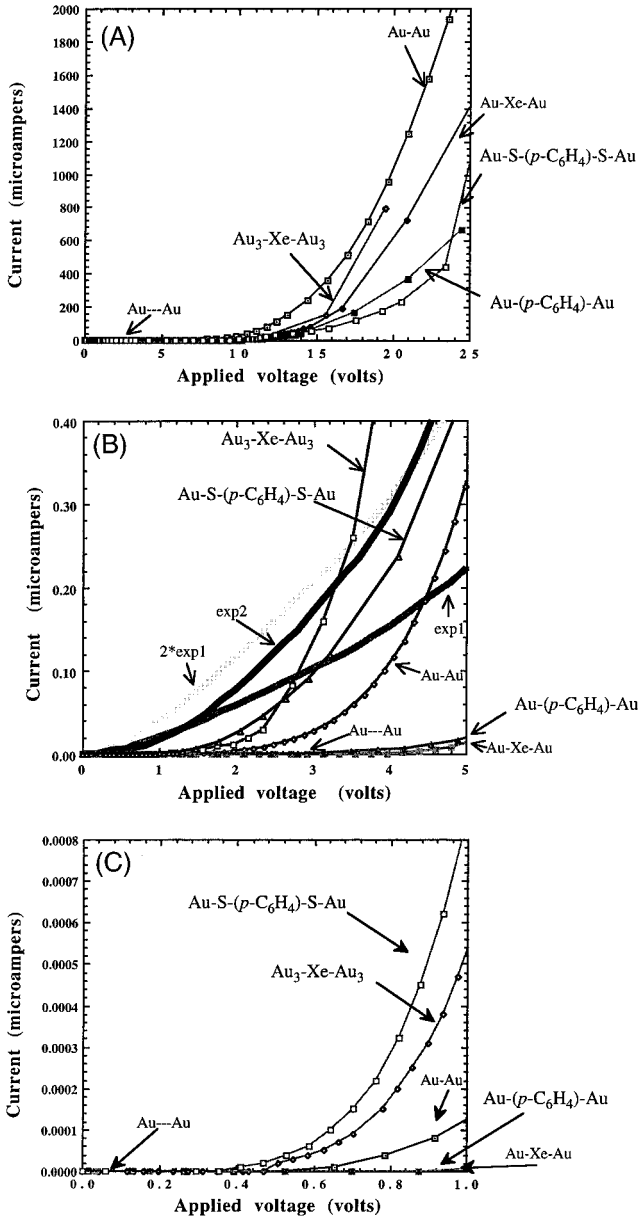

Figure 4. Molecular $I(V)$ characteristics for the systems Au−Au, Au−Xe−Au, Au_3−Xe−Au_3, Au−(*p*-C_6H_4)−Au, and Au−S−(*p*-C_6H_4)−S−Au: (A) 0−25 V range; (B) 0−10 V range; (C) 0−1 V range. In part B, exp1 and exp2 correspond to the experimentally determined values (ref 1) of $I(V)$ for one Au−S−(*p*-C_6H_4)−S−Au and two parallel Au−S−(*p*-C_6H_4)−S−Au systems, respectively, while "2*exp1" corresponds to the mathematical doubling of the results from exp1.

connected to the Au atoms through heteroatom connects ("alligator clips") such as sulfur, these present a barrier effect. For larger input fields, however, the situation is very similar to the case when the molecule is directly connected to the Au atoms without the sulfur units. With the direct connection to the aryl ring, there is practically no barrier observed, however the conductances are much smaller. In the absence of bridging molecules, the Au tips would not conduct electrons except at very high fields. This computational technique could be used with no bias data from experimentally derived results; therefore, it can guide future experimental approaches to molecular scale electronic junctions.

Acknowledgment. Support came from the Defense Advanced Research Projects Agency and the Office of Naval Research (N00014-97-1-0806, N00014-99-1-0406). We thank NASA for the use of their supercomputing facilities, Dr. M. J. Frisch of Lorentzian, Inc. and Prof. E. K. U. Gross for helpful discussions.

References and Notes

(1) Reed, M. A.; Zhou, C.; Muller, C. J.; Burgin, T. P. Tour, J. M. *Science* **1997**, *278*, 252−254.

(2) Crommie, M. F.; Lutz, C. P.; Eigler, D. M. *Phys. Rev. B* **1993**, *48*, 2851−2854.

(3) Joachim, C.; Gimzewski, J. K.; Schlittler, R. R.; Chavy, C. *Phys. Rev. Lett.* **1995**, *74*, 2102−2105.

(4) (a) Yazdani, A.; Eigler, D. M.; Lang, N. D. *Science* **1996**, *272*, 1921−1924. (b) Lang, N. D. *Phys. Rev. B* **1995**, *52*, 5335.

(5) Seminario, J. M.; Tour, J. M. *Int. J. Quantum Chem.* **1997**, *65*, 749−758.

(6) Seminario, J. M.; Zacarias, A. G.; Tour, J. M. *J. Am. Chem. Soc.* **1998**, *120*, 3970−3974.

(7) Seminario, J. M. In *Computational Chemistry and Chemical Engineering*; Cisneros, G.; Cogordan, J. A.; Castro, M., Wang, C., Eds.; World Scientific: Singapore, 1997; pp 255−267.

(8) Joachim, C.; Gimzewski, J. K. *Chem. Phys. Lett.* **1997**, *256*, 353−357.

(9) Aviram, A.; Ratner, M. A. *Chem. Phys. Lett.* **1974**, *29*, 277.

(10) Davis, W. B.; Wasiliewski, M. R.; Ratner, M. A.; Mujica, V.; Nitzan, A. *J. Phys. Chem. A* **1997**, *101*, 6158−6164.

(11) Mujica, V.; Kemp, M.; Ratner, M. A. *J. Chem. Phys.* **1994**, *101*, 6856−6864.

(12) Mujica, V.; Kemp, M.; Roitberg, A. M. R. *J. Phys. Chem.* **1996**, *104*, 7296−7305.

(13) Datta, S. *Electronic Transport in Mesoscopic Systems*; Cambridge University Press: Cambridge, U.K., 1995.

(14) Datta, S.; Tian, W.; Hong, S.; Reifenberger, R.; Henderson, J.; Kubiak, C. P. *Phys. Rev. Lett.* **1997**, *79*, 2530−2533.

(15) *Modern Density Functional Theory: A Tool for Chemistry*; Seminario, J. M., Politzer, P., Eds.; Elsevier: Amsterdam, 1995; p 405.

(16) *Recent Developments and Applications of Modern Density Functional Theory*; Seminario, J. M., Ed.; Elsevier: Amsterdam, 1996; p 900.

(17) Parr, R. G.; Yang, W. *Density Functional Theory of Atoms and Molecules*; Oxford University Press: Oxford, 1989.

(18) Kryachko, E. S.; Ludeña, E. *Energy Density Functional Theory of Many-Electron Systems*; Academic: New York, 1990.

(19) Becke, A. D. *J. Chem. Phys.* **1993**, *98*, 5648−5652.

(20) Perdew, J. P. In *Electronic Structure of Solids*; Ziesche, P., Eschrig, H. Eds.; Akademie Verlag: Berlin, 1991; pp 11−20.

(21) Dunning Jr., T. H.; Hay, P. J. In *Methods of Electronic Structure Theory*; Shaefer, H. F., III, Eds.; Plenum: New York, 1976; Vol. 3, pp 1−28.

(22) Hay, P. J.; Wadt, W. R. *J. Chem. Phys.* **1985**, *82*, 299−310.

(23) Neyman, K. M.; Pacchioni, G.; Rösch, N. In *Recent Developments and Applications of Modern Density Functional Theory*; Seminario, J. M., Eds.; Elsevier: Amsterdam, 1996; pp 569−619.

(24) Görling, A.; Levy, M. *J. Chem. Phys.* **1997**, *106*, 2675−2680.

(25) Frisch, M. J.; Trucks, G. W.; Schlegel, H. B.; Gill, P. M. W.; Johnson, B. G.; Robb, M. A.; Cheeseman, J. R.; Keith, T.; Petersson, G. A.; Montgomery, J. A.; Raghavachari, K.; Al-Laham, M. A.; Zakrzewski, V. G.; Ortiz, J. V.; Foresman, J. B.; Ciolowski, J.; Stefanov, B. B.; Nenayakkara, A.; Challacombe, M.; Peng, C. Y.; Ayala, P. Y.; Chen, W.; Wong, M. W.; Andres, J. L.; Replogle, E. S.; Gomperts, R.; Martin, R. L.; Fox, D. J.; Binkley, J. S.; Defrees, D. J.; Baker, J.; Stewart, J. P.; Head-Gordon, M.; Gonzalez, C.; Pople, J. A. *Gaussian 94*; E.1 version; Gaussian, Inc.: Pittsburgh, PA, 1996.

(26) Peng, C.; Ayala, P. Y.; Schlegel, H. B.; Frisch, M. J. *J. Comput. Chem.* **1996**, *17*, 49−56.

(27) Merzbacher, E. *Quantum Mechanics*; Wiley & Sons: New York, 1974.

(28) Mulliken, R. S. *J. Chem. Phys.* **1955**, *23*, 1833, 1841, 2338, 2343.

(29) Breneman, C. M.; Wiberg, K. B. *J. Comput. Chem.* **1990**, *11*, 361−373.

(30) Lang, E.; Grimm, W.; Heinz, K. *Surf. Sci.* **1982**, *117*, 169−179.